Supporting Information

Bareyre et al. 10.1073/pnas.1015239108

SI Materials and Methods

AAV Vector Construction, Production, and Purification. The adeno-associated viral vectors used in this study have been cloned into the pAAV-MCS vector from Stratagene as follows. Briefly, for the control pAAV-*ires*-GFP vector, a strong modified internal ribosome entry site (*ires*) of the encephalomyocarditis virus, which permits the translation of two genes of interest from a single bicistronic mRNA, was cut with BamHI and BstXI from the pires2-DsRed2 plasmid (Clontech) and inserted at the HincII site of pAAV-MCS. Then the DNA coding for GFP was inserted at the XhoI site of pAAV-MCS to create the pAAV-*ires*-GFP construct. The pAAV-Cre-*ires*-GFP construct was cloned by excising the coding sequence for Cre recombinase from pBS185 (gift of Thomas Hughes, Montana State University, MT) with XhoI and MluI and inserting it into the EcoRI site of pAAV-*ires*-GFP. For the pAAV-STAT3, the STAT3 gene was excised from pcDNA3 STAT3 (Addgene plasmid 8706) with BamHI and XhoI and cloned in the pAAV-MCS at the HincII site. For cloning the pAAV-STAT3c, the STAT3c gene was excised from pRc/CMV STAT3c Flag (Addgene plasmid 8722) with NotI and SwaI and inserted in the HincII site of pAAV-MCS. Control pAAV-eCFP was engineered by excising the eCFP gene from the peCFP N1 plasmid at BamHI and NotI and cloning it in the pAAV-MCS at the HincII site.

AAV serotype 2 particles were then produced in HEK293 cells by the adenovirus-free AAV production method (1, 2). Briefly, HEK293 cells were seeded at 80% confluence and cotransfected using the calcium phosphate method with 7.5 μg of pRC (3), 7.5 μg of transgene plasmid, and 22.5 μg of pXX6 (1, 2). After 48 h, cells were harvested and pelleted by low-speed centrifugation. Cells were resuspended in 150 mM NaCl/50 mM Tris-HCl (pH 8.5), freeze/thawed three times, and treated with Benzonase (50 U/mL lysate) for 30 min at 37 °C. To purify viral vector preparations, cell debris was removed by centrifugation at 3,700 × *g* for 20 min at 4 °C, and the supernatant was loaded onto a discontinuous iodixanol gradient (3). Following harvesting of the 40% phase, a heparin affinity chromatography was conducted. Briefly, a heparin affinity column (HiTrap heparin HP; GE Healthcare) was equilibrated with 1× PBS solution/$MgCl_2$ (1 mM)/KCl (2.5 mM). The vector solution was diluted 1:10 in the same buffer and applied to the column. After a washing step with 1× PBS solution/$MgCl_2$ (1 mM)/KCl (2.5 mM), the vector was eluted with 1× PBS/$MgCl_2$ (1 mM)/KCl (2.5 mM) plus 1 M NaCl in 500-μL steps.

To determine the genomic particle titer, vector genomes were isolated by DNeasy Tissue Kit (Qiagen) and subjected to quantitative PCR analysis by using the LightCycler rapid thermal cycler system (Roche Diagnostics) and the SYBR Green kit (Roche Diagnostics). Genomic titers were as follows: rAAV-STAT3, 9×10^{12} genome copies/mL; rAAV-STAT3c, 5.5×10^{12} genome copies/mL; rAAV-eCFP, 9.2×10^{12} genome copies/mL; rAAV-Cre, 9×10^{12} genome copies/mL; rAAV-Cre-*ires*-GFP, $5.7–7.1 \times 10^{11}$ genome copies/mL; and rAAV-*ires*-GFP, $1.4–3.8 \times 10^{12}$ genome copies/mL.

Tissue Processing, Immunohistochemistry, and STAT Expression Analysis. Animals were deeply anesthetized with isoflurane and perfused transcardially with saline solution followed by 4% paraformaldehyde in 0.01 M phosphate buffer. Tissues were postfixed in 4% paraformaldehyde at 4 °C for 24 h. For immunofluorescence analysis, DRGs were dissected out, transferred to 30% sucrose for at least 24 h, and embedded in Tissue-Tek optimal cutting temperature compound (Sakura Finetek). Then, 20-μm-thick coronal sections were cut on a cryostat. Immunofluorescence staining of DRG sections was performed as described previously (4). Before immunostaining, sections were heated in a microwave to improve antigen retrieval. Antibodies were diluted in a working solution of PBS containing 0.2% Triton X-100 (Sigma) and 10% normal horse serum (Jackson Laboratory), and incubation was performed at room temperature or at 4 °C overnight. Details of the primary antibodies are as follows: STAT3 (dilution 1:500; Cell Signaling), P-STAT3 (dilution 1:50; Cell Signaling), and cJun (dilution 1:500; Santa Cruz Biotechnology). Secondary antibodies (goat anti-rabbit 594, goat anti-rabbit 488) were obtained from Jackson Laboratory and used at a dilution of 1:500. Nuclei were counterstained using NeuroTrace 435 (Invitrogen) and mounted in Vectashield (Vector Laboratories).

P-STAT3 and STAT3 immunoreactivity was analyzed in L3 DRGs of animals perfused at 1 h, 6 h, 2 d, 1 wk, and 2 wk after a bilateral saphenous nerve transection. P-STAT3 immunoreactivity was also analyzed in L3 DRGs of mice perfused 1 h, 6 h, 2 d, 1 wk, and 2 wk after the saphenous nerve was double-crushed with hand-held forceps. Immunofluorescence analysis of cJun induction in DRG neurons and confocal microscopy analysis of Wallerian degeneration in distal nerve segments of Thy1-YFP[16] mice were used to confirm the success of the crush lesion (Fig. S5). P-STAT3 and STAT3 immunoreactivity was further analyzed in C6 DRGs of animals perfused at 1 h, 6 h, 2 d, 1 wk, and 2 wk after a bilateral dorsal column lesion. For the dorsal column lesion, animals were anesthetized with isoflurane, and a dorsal laminectomy was performed at the C4 to C6 spinal cord level as previously described (4). A small incision was made in the dura, and the dorsal column was then cut with fine iridectomy scissors. Unlesioned animals were used as controls. All DRG sections were counterstained with NeuroTrace 435 (as described earlier) to reveal the total number of neuronal nuclei in the DRG, and the proportion of DRG neurons showing STAT3 or P-STAT3 immunoreactivity was determined.

In Situ Analysis of Peripheral Axon Regeneration. To evaluate the regeneration of peripheral DRG branches, $STAT3^{fl/fl}$ mice (5) injected with rAAV-Cre-*ires*-GFP or rAAV-*ires*-GFP were transcardially perfused with 4% paraformaldehyde at 4 or 14 d after saphenous nerve transection. Cross-sections of the saphenous nerve were cut rostrally to the injury site to quantify the number of GFP-labeled axons above the lesion. The distal part of the nerve containing the lesion site was dissected with the surrounding muscular tissue and flat-mounted in Vectashield (Vector Laboratories). High-resolution image stacks of the axons were taken on a FV 1000 confocal microscope system (Olympus). Then lines were positioned on the confocal maximum intensity projections at 0.1 mm, 0.2 mm, 0.4 mm, 0.8 mm, 1.4 mm, 2 mm, and 5 mm distal from the lesion site (Fig. 1*H*). The number of axons crossing these lines was counted. A ratio of regenerating axons was calculated by dividing the number of regenerating axons at a given distances from the lesion by the number of labeled axons rostral to the lesion.

To determine the percentage of DRG neurons that reach the proximity of their original target area, retrograde tracing experiments were performed as follows: At 28 d following the SNC, a gel foam impregnated with the tracer Miniruby (Invitrogen) was applied to the distal-most part of the saphenous nerve (located approximately 10 mm distal to the cut nerve). Three days later, mice were deeply anesthetized and transcardially perfused with PFA. Then, L3 DRGs were dissected and 20-μm sections

were cut on the cryostat as described earlier. Confocal images of the sections were acquired on an Olympus FV 1000 confocal microscope and the number of Miniruby-positive DRG neurons and total DRG neurons (identified by costaining with NeuroTrace 435) were counted. The percentage of Miniruby-positive DRG neurons was calculated and normalized to the percentage of Miniruby-positive neurons that were retrogradely traced from the same anatomical localization in unlesioned mice (45 ± 6% of Miniruby-positive L3 DRG neurons; $n = 14$ sections, $n = 2$ mice). Mice traced from the same anatomical localization immediately after the saphenous nerve was cut showed no labeling, indicating that the labeling at 28 d is caused by long-distance regeneration.

To determine whether the overexpression of STAT3 or STAT3c could increase peripheral axon regeneration, we injected 1 μL of rAAV-STAT3, rAAV-STAT3c, or rAAV-Cre (control rAAV) into the L3 DRG of *Thy1*-YFP[16] mice (6), in which a large proportion of DRG neurons are fluorescently labeled with the YFP. We then performed an SNC and evaluated axonal sprouting and regeneration at 4 d after the lesion as described earlier.

In Vivo Analysis of Peripheral Axon Regeneration. For in vivo imaging experiments, we used sparsely labeled animals, lesioned the saphenous nerve as described earlier, and marked the position of the axons proximally and distally from the lesion site with a suspension of 1-μm-diameter orange FluoSpheres (Invitrogen). Before each imaging session, animals were anesthetized and placed directly under a fluorescence dissection microscope (Olympus). An incision was made on top of the lesion site and the axons in the saphenous nerve were imaged with 20× magnification at day 2 and 3 or at day 7 and 8 after lesion. Images were captured with a cooled Sensicam QE CCD camera (pco.imaging). To determine the growth of the transected axon ends, we measured the distance from the axon end to the FluoSpheres proximal to the lesion site at 2 and 3 d or 7 and 8 d after lesion and calculated the speed of growth per day.

In Vivo and in Situ Analysis of Central Axon Outgrowth. To image central branches of fluorescently labeled DRG neurons, we adapted our previously established spinal in vivo imaging approach (4). Briefly, *Thy1*-GFP^{s} mice were anesthetized by an i.p. injection of ketamine/xylazine. To access the cervical spinal cord, a laminectomy was performed and the dorsal surface of the spinal cord was exposed. During the imaging session, the spinal cord was superfused with mouse artificial cerebrospinal fluid. To follow the outgrowth of individual axons in vivo, we first identified single fluorescently labeled axons emerging from a DRG using a widefield set-up based on an Olympus BX51 microscope equipped with ×4/0.13 dry, ×10/0.3 dry, and ×20/0.5 dipping cone water-immersion objectives. To document these axons in vivo, image streams of 25 to 50 images were acquired with a cooled Sensicam QE CCD camera controlled by MetaMorph software as previously described (4). The DRG from which the selected axon was emerging was then surgically prepared and 1 μL of one of the rAAVs was injected by using a glass capillary as described earlier. Then, 10 to 12 d after the DRG injection, the dorsal surface of the spinal cord was surgically reexposed. The previously identified axon was transected by using a hand-held small-diameter needle and documented in vivo. Two different imaging protocols were used as follows.

To determine the frequency of axonal sprouting, the animal was perfused transcardially with 4% PFA 2 d after the lesion and the previously imaged spinal cord segment was dissected. The transected axon was then documented by using high-resolution confocal microscopy as described earlier, first in the intact spinal cord and then in 100- to 250-μm-thick vibratome sections. Confocal stacks were processed as described earlier and the transected axons were reconstructed from the DRG root to the lesion site. Axons were then evaluated by two blinded observers and terminal axon ends were classified as "sprouts" or "bulbs" based on their characteristic morphological appearances. Further, the number of collateral sprouts emerging from the transected axons was counted.

To determine the speed of axonal outgrowth we reimaged the transected axon ends at 2 and 4 d after lesion in vivo using a custom-built multiphoton imaging setup based on an Olympus FV 300 scanner equipped with a femtosecond pulsed Ti:Sapphire laser (Mai Tai HP; Newport/Spectra-Physics). We acquired image stacks of 50 to 200 images per stack (spaced at 1–2 μm in z dimension) for each frame with a ×20/0.5 dipping cone water-immersion objective. Animals were then perfused transcardially with 4% PFA 10 d after the lesion. The imaged part of the spinal cord was dissected out. The transected axons were reidentified in the fixed tissue and imaged in the intact spinal cord by using an Olympus FV1000 MPE multiphoton microscope or an Olympus FV1000 confocal microscope. Image stacks of 20 to 100 frames were acquired with a ×25/1.05 water-immersion or a ×20/0.85 oil-immersion objective. Imaging stacks were processed by using MetaMorph or ImageJ/Fiji software. Frames containing the axon were selected, and the transected axons were reconstructed using Photoshop. To determine the growth of the transected axon ends, we measured the distance from the axon end to a characteristic proximal structure (in most cases the Y-branch point in the dorsal root; in some cases a crossing point with another axon) at 2, 4, and 10 d after lesion. To compensate for tissue changes caused by fixation in the perfused samples, we measured a "constant" distance e.g., between two branch points in the same unlesioned axon both in vivo and in the corresponding fixed tissue to determine a sample-specific "correction factor." The length of the transected axon end measured in fixed tissue was then multiplied by this correction factor. Axons that showed substantial die-back were excluded from the analysis.

To determine the influence of endogenous STAT3 expression on axonal sprouting after a CNS lesion, we injected 1 μL of rAAV-eCFP or a combination of rAAV-eCFP and rAAV-Cre into the cervical DRGs of STAT3$^{fl/fl}$ mice. Ten days after the injection, fluorescently labeled spinal DRG axons were lesioned by a pin as described earlier. Then, 2 d following the lesion, animals were perfused and axonal sprouting was evaluated based on confocal stacks of the fixed intact spinal cord as described earlier.

To determine the effects of a combination therapy with STAT3 and chondroitinase ABC, we performed the following experiment. We first injected 1 μL of rAAV-STAT3 or rAAV-Cre into the cervical DRGs of *Thy1*-GFP^{s} mice as described earlier. Ten days after this injection, we then lesioned individual GFP-positive spinal axons and administered a first bolus of 6 μL of chondroitinase ABC (10 U/mL in saline solution with 0,01% BSA; Sigma-Aldrich) or vehicle only (saline solution with 0.01% BSA) immediately following lesion creation. At the same time, an osmotic minipump (1007B; Alzet), which was connected to a brain infusion kit (Alzet) inserted into the lateral ventricle, was installed and started to deliver 0.5 μL/h of chondroitinase ABC (10 U/mL in saline solution with 0.01% BSA) or vehicle only for 7 d. At 10 d following the lesion, the animals were perfused with PFA, the spinal cords were dissected, and the transected axons were imaged in the intact fixed spinal cord by confocal microscopy as described earlier. On confocal image stacks, we then measured the length of axonal sprouts to determine the axonal outgrowth (axonal terminals that ended in tips or bulbs were considered to be nongrowing axons and their outgrowth was set to 0 μm).

1. Zolotukhin S, et al. (1999) Recombinant adeno-associated virus purification using novel methods improves infectious titer and yield. *Gene Ther* 6:973–985.
2. Zhang HG, et al. (2000) Adeno-associated virus production of soluble tumor necrosis factor receptor neutralizes tumor necrosis factor alpha and reduces arthritis. *Hum Gene Ther* 11:2431–2442.
3. Girod A, et al. (1999) Genetic capsid modifications allow efficient re-targeting of adeno-associated virus type 2. *Nat Med* 5:1052–1056.
4. Kerschensteiner M, Schwab ME, Lichtman JW, Misgeld T (2005) In vivo imaging of axonal degeneration and regeneration in the injured spinal cord. *Nat Med* 11:572–577.
5. Matsukawa A, et al. (2003) Aberrant inflammation and lethality to septic peritonitis in mice lacking STAT3 in macrophages and neutrophils. *J Immunol* 171:6198–6205.
6. Feng G, et al. (2000) Imaging neuronal subsets in transgenic mice expressing multiple spectral variants of GFP. *Neuron* 28:41–51.

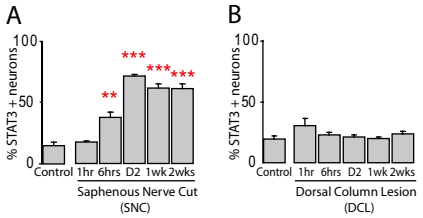

Fig. S1. Induction of STAT3 expression by a peripheral nerve cut but not by a central lesion. (*A*) Quantification of the number of STAT3-positive DRG neurons (identified by NeuroTrace counterstaining) at different time points following SNC in WT mice. (*B*) Quantification of the number of STAT3-positive DRG neurons (identified by NeuroTrace counterstaining) at different time points following DCL in WT mice.

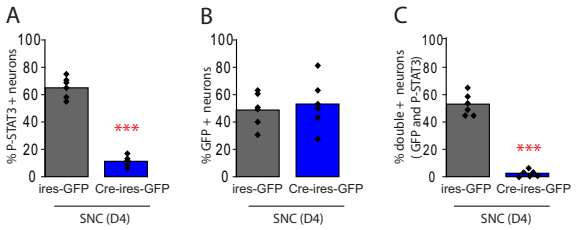

Fig. S2. rAAV-Cre-*ires*-GFP is an efficient tool to delete STAT3 and concomitantly express GFP in DRG neurons. (*A* and *B*) Quantification of the percentage of P-STAT3–positive (*A*, also shown in Fig. 1*E*) and GFP-positive (*B*) neurons 4 d following SNC in DRGs of STAT3$^{fl/fl}$ mice previously injected with rAAV-*ires*-GFP (gray columns) or rAAV-Cre-*ires*-GFP (blue columns; n = 6 animals per group). Although GFP expression is comparable in both groups of DRGs, only injection of the rAAV-Cre-*ires*-GFP leads to a significant reduction of P-STAT3 expression. P-STAT3 expression is reduced by approximately 80% in DRG neurons, whereas only 50% of the neurons express GFP. This is expected because of the lower expression rate of the second reading frame, which encodes GFP, and the low number of Cre molecules needed to ensure efficient excision of floxed sequences. (*C*) Analysis of P-STAT3 expression in GFP-positive DRG neurons confirms that P-STAT3 expression is completely abolished in DRG neurons infected with rAAV-Cre-*ires*-GFP.

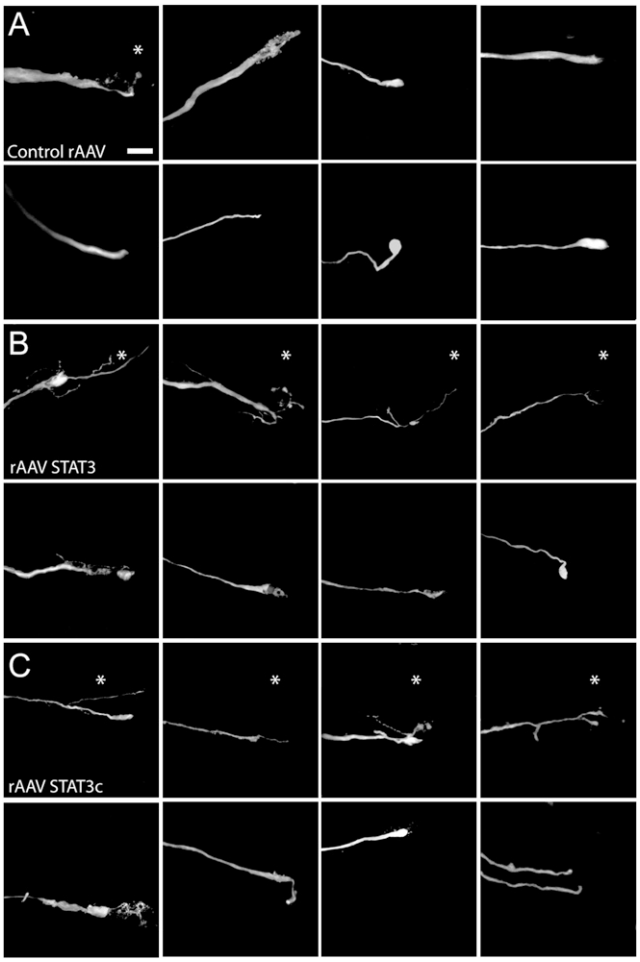

Fig. S3. Gallery of central DRG axon endings after treatment with control rAAV, rAAV-STAT3, and r-AAV-STAT3c. (*A*–*C*) Representative images of axon endings 2 d after a central lesion derived from DRG neurons treated with control rAAV (*A*), rAAV-STAT3 (*B*), or rAAV-STAT3c (*C*). Axonal sprouts (asterisks) are rarely found in control axons (*A*) but are frequent in axons emerging from DRG neurons expressing STAT3 (*B*) or STAT3c (*C*). (Scale bar: *A*, 25 μm.)

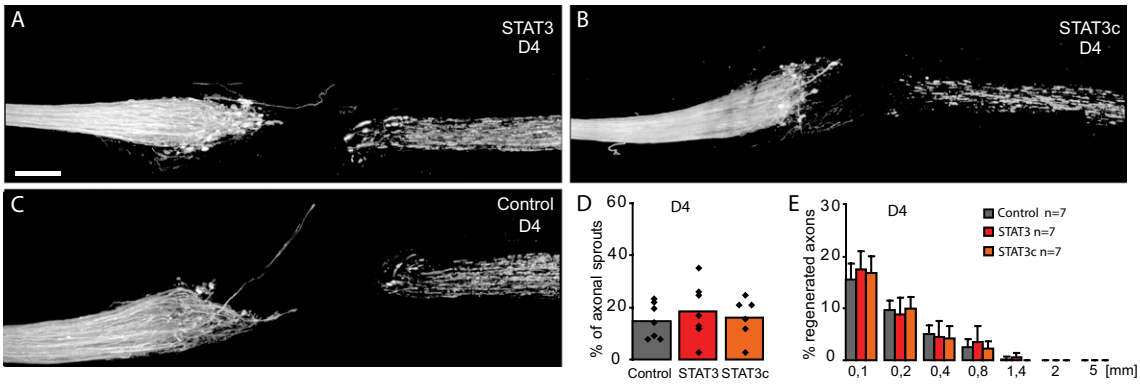

Fig. S4. Overexpression of STAT3 or STAT3c does not increase peripheral axon regeneration following a SNC. (*A*–*C*). Confocal images taken at 4 d after SNC displaying the proximal stump of saphenous nerve that receives fibers from L3 DRGs injected with rAAV-STAT3 (*A*), rAAV-STAT3c (*B*), or control rAAV (*C*). Axons are fluorescently labeled with YFP (white) in *Thy1*-YFP[16] mice. (*D* and *E*) Quantification of axonal sprouting at the site of the lesion (*D*) and regeneration ratios (*E*) at different distances from the cut site (Fig. 1*H*) of axons derived from DRG neurons that express normal levels of STAT3 (gray columns) or overexpress STAT3 (red columns) or STAT3c (orange columns) at 4 d after SNC. (Scale bar: *A*, 250 μm.)

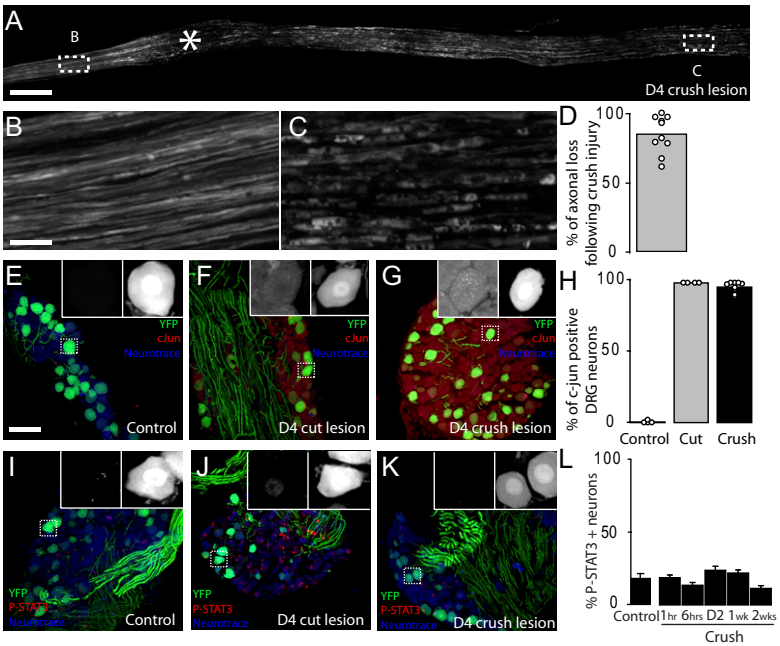

Fig. S5. A peripheral crush lesion leads to Wallerian degeneration and induces cJun expression but not STAT3 activation in DRG neurons (*A*–*C*) Wallerian degeneration of axons (white) in the distal stump of a saphenous nerve 4 d following saphenous nerve crush in *Thy1*-YFP[16] mice. Magnification of the areas boxed in *A* shows intact axons rostral to the lesion (*B*) and axonal fragments distal to the lesion (*C*). (*D*) Quantification of the loss of continuous axons distal to the lesion at 4 d after injury. (*E*–*G*) Confocal images illustrating cJun immunoreactivity (red) in an unlesioned control DRG (*E*), and in DRGs following saphenous nerve cut (*F*) or crush (*G*; YFP, green; NeuroTrace, cyan). (*H*) Quantification of the number of cJun-positive L3 DRG neurons (identified by NeuroTrace counterstaining) in unlesioned controls and 4 d following saphenous nerve cut or crush. (*I*–*K*) Confocal images illustrating P-STAT immunoreactivity (red) in an unlesioned control DRG (*I*) and in DRGs following saphenous nerve cut (*J*) and crush (*K*; YFP, green; NeuroTrace, cyan). (*L*) Quantification of the number of P-STAT3–positive DRG neurons (identified by NeuroTrace counterstaining) at different time points following saphenous nerve crush in WT mice. (Scale bars: *A*, 400 μm; *B*, 40 μm; *E*, 100 μm.)